

Inferior Olivary Neurons Innervate Multiple Zones of the Flocculus in Pigeons (*Columba livia*)

JANELLE M.P. PAKAN,¹ KATHRYN G. TODD,¹⁻³ ANGELA P. NGUYEN,¹
 IAN R. WINSHIP,⁴ PETER L. HURD,⁴ LAUREN L. JANTZIE,^{2,3}
 AND DOUGLAS R.W. WYLIE^{1,4*}

¹Division of Neuroscience, University of Alberta, Edmonton, Alberta T6G 2E9, Canada

²Neurochemical Research Unit, University of Alberta, Edmonton, Alberta T6G 2E9, Canada

³Department of Psychiatry, University of Alberta, Edmonton, Alberta T6G 2E9, Canada

⁴Department of Psychology, University of Alberta, Edmonton, Alberta T6G 2E9, Canada

ABSTRACT

Complex spike activity of floccular Purkinje cells responds to patterns of rotational optic flow about the vertical axis (*rVA* neurons) or a horizontal axis 45° to the midline (*rH45* neurons). The pigeon flocculus is organized into four parasagittal zones: two *rVA* zones (zones 0 and 2) interdigitated with two *rH45* zones (zones 1 and 3). Climbing fiber input to the *rVA* and *rH45* zones arises in the caudal and rostral regions of the medial column of the inferior olive (mcIO), respectively. To determine whether the two *rVA* zones and the two *rH45* zones receive input from different areas of the caudal and rostral mcIO and whether individual neurons project to both zones of the same rotational preference, different colors of fluorescent retrograde tracer were injected into the two *rVA* or two *rH45* zones. For the *rVA* injections, retrogradely labeled cells from the two zones were intermingled in the caudal mcIO, but the distribution of cells labeled from zone 0 was slightly caudal to that from zone 2. On average, 18% of neurons were double labeled. For the *rH45* injections, cells retrogradely labeled from the two zones were intermingled in the rostral mcIO, but the distribution of cells labeled from zone 1 was slightly rostral to that from zone 3. On average, 22% of neurons were double labeled. In sum, each of the two *rVA* zones and the two *rH45* zones receives input from slightly different regions of the mcIO, and about 20% of the neurons project to both zones. *J. Comp. Neurol.* 486:159–168, 2005. © 2005 Wiley-Liss, Inc.

Indexing terms: optokinetic; optic flow; vestibulocerebellum; climbing fibers; cholera toxin subunit B; fluorescent tracers

The flocculus of the vestibulocerebellum is involved in the control of gaze stabilization. The complex spike activity (CSA) of floccular Purkinje cells responds best to patterns of optic flow that result from self-rotation about one of two axes in three-dimensional space: either the vertical axis or a horizontal axis oriented at 45° contralateral azimuth/135° ipsilateral azimuth (Simpson et al., 1981; Graf et al., 1988; Wylie and Frost, 1993). We refer to these two response types as *rVA* and *rH45* neurons, respectively (Winship and Wylie, 2003; Wylie et al., 2003; Voogd and Wylie, 2004). These response types were first shown in rabbits by Simpson, Graf, and colleagues (Simpson et al., 1981, 1988a,b, 1989a,b; Graf et al., 1988; see also Leonard et al., 1988), who emphasized that the rotational optokinetic system is organized with respect to a three-axis reference frame that is common to the vestibular canals and the eye muscles (Simpson and Graf,

1981, 1985; Ezure and Graf, 1984; Graf et al., 1988; Leonard et al., 1988; Simpson et al., 1988a,b, 1989a,b;

Grant sponsor: Natural Sciences and Engineering Research Council of Canada (to J.M.P.P., I.R.W.); Grant number: 170363 (to D.R.W.W.); Grant sponsor: Canadian Institute for Health Research; Grant number: 69013 (to D.R.W.W.); Grant number: 49622 (to K.G.T.); Grant sponsor: Davey Endowment for Brain Injury Research (to K.G.T.); Grant sponsor: Alberta Heritage Foundation for Medical Research (to J.M.P.P. and I.R.W.); Grant sponsor: Canada Research Chairs Program (to D.R.W.W.).

*Correspondence to: Douglas R.W. Wylie, Department of Psychology, University of Alberta, Edmonton, Alberta Canada T6G 2E9. E-mail: dwylie@ualberta.ca

Received 6 October 2004; Revised 2 December 2004; Accepted 20 January 2005

DOI 10.1002/cne.20523

Published online in Wiley InterScience (www.interscience.wiley.com).

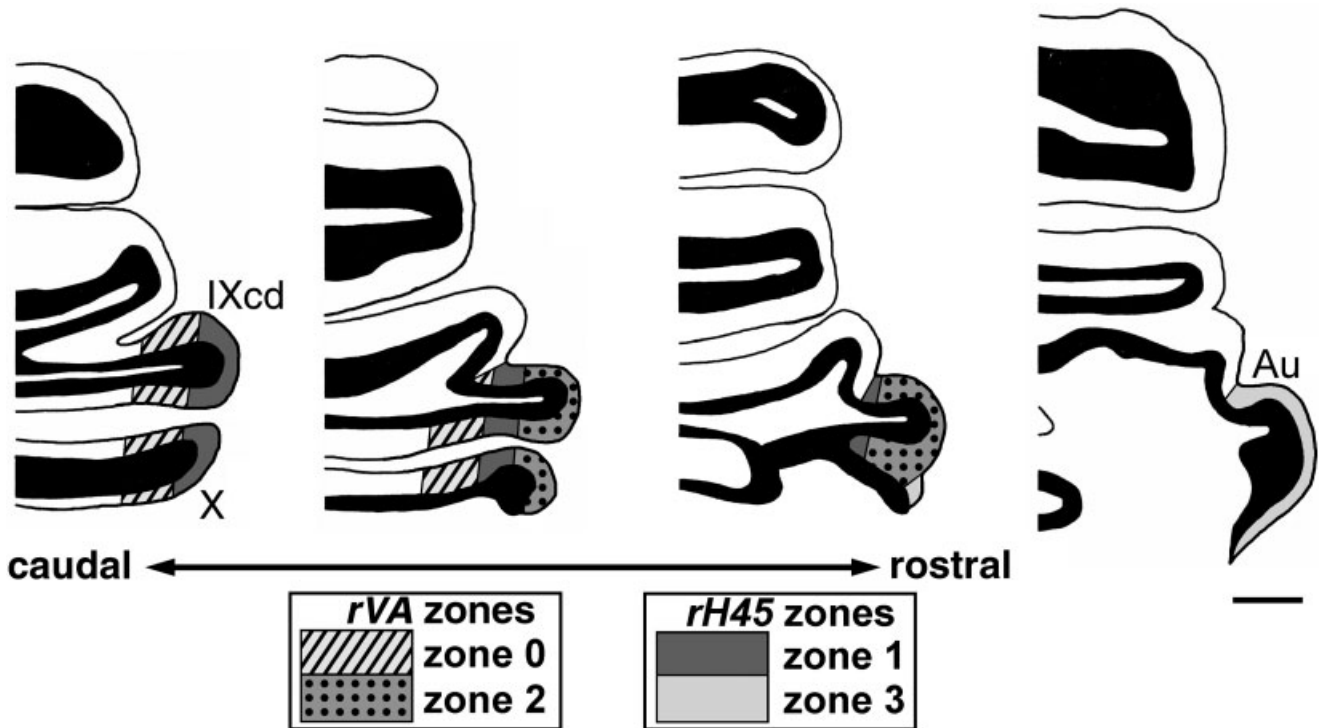


Fig. 1. Zonal organization of the pigeon flocculus. The approximate boundaries of the *rVA* and *rH45* optic flow zones were superimposed on a series of tracings through the vestibulocerebellum based on climbing fiber labeling (Winship and Wylie, 2003) and supported by electrophysiological recordings (Wylie et al., 2003). Caudally to rostrally, each section is approximately 0.5 mm apart. Scale bar = 1 mm.

van der Steen et al., 1994; see also Wylie and Frost, 1996; Wylie et al., 1998).

In several species, it has been shown that the *rVA* and *rH45* cells are organized into interdigitated parasagittal zones. The order of the zones in the pigeon flocculus is shown in Figure 1. There are four parasagittal zones: two *rVA* zones and two *rH45* zones. The caudomedial most zone is an *rVA* zone, zone 0. This is followed successively by *rH45* zone 1, *rVA* zone 2, and finally the rostralateral most zone 3, an *rH45* zone. These correspond to zones 0–3 of the rat cerebellum (Sugihara et al., 2004; Voogd and Wylie, 2004; see Discussion). The climbing fiber (CF) input to the *rVA* and *rH45* zones arises in the caudal and rostral regions of the medial column of the inferior olive (mcIO), respectively (Wylie et al., 1999; Winship and Wylie, 2003). In the present study, we used fluorescent retrograde trac-

ers to investigate the CF input to the zones of the pigeon flocculus. We had three aims: 1) to determine whether the two different *rVA* zones receive input from different areas of the caudal mcIO; 2) to determine whether the two different *rH45* zones receive input from different areas of the rostral mcIO; and 3) to assess whether individual olivary neurons project to both *rVA* zones or both *rH45* zones.

MATERIALS AND METHODS

The methods reported herein conformed to the guidelines established by the Canadian Council on Animal Care and were approved by the Biosciences Animal Care and Policy Committee at the University of Alberta. Silver king and homing pigeons, obtained from a local supplier, were anesthetized by intramuscular injection of a ketamine (65 mg/kg)/xylazine (8 mg/kg) cocktail. Supplemental doses were administered as necessary. Animals were placed in a stereotaxic device with pigeon ear bars and a beak bar adapter so that the orientation of the skull conformed to the atlas of Karten and Hodós (1967). To access the flocculus, the bone surrounding the semicircular canals was removed, because the dorsal surface of the flocculus (folium IXcd) lies within the radius of the anterior semicircular canal. This exposure allows easy access to the two *rVA* zones (zones 0 and 2) and the two *rH45* zones (zone 1 and 3). The dura was removed, and a glass micropipette (4–5 μm tip diameter) containing 2 M NaCl was advanced into the flocculus with a hydraulic microdrive (Fredrick

Abbreviations

Au	auricle
CbL	lateral cerebellar nucleus
dl	dorsal lamella of the inferior olive
IO	inferior olive
mcIO	medial column of the inferior olive
MLF	medial longitudinal fasciculus
R	raphe
VeM	medial vestibular nucleus
vl	ventral lamella of the inferior olive
IX	folium IX
X	folium X
XII	hypoglossal nerve

Haer & Co.) in order to make extracellular recordings of Purkinje cell CSA. The optic flow preference of isolated CSA was identified by moving a large hand-held stimulus (90° x 90°) in various areas of the visual field. *rVA* and *rH45* neurons are easily distinguished with this procedure: *rVA* neurons respond best to forward (temporal to nasal) motion in the ipsilateral eye and backward motion in the contralateral eye, whereas *rH45* neurons prefer upward motion in the ipsilateral visual field and the anterior quadrant of the contralateral visual field and downward motion in the posterior three quarters of the contralateral visual field (Simpson et al., 1981; Graf et al., 1988; Wylie and Frost, 1993; Winship and Wylie, 2001). Several penetrations were made to map out the locations of zones. Subsequently, the recording electrode was replaced with a micropipette (20 μ m tip diameter) containing a 1% cholera toxin subunit-B (CTB)-AlexaFluor 488 or 594 conjugate (Molecular Probes, Eugene, OR), except for case *rH45-4*, in which green and red fluorescent latex microspheres (Lumafuor Corp., Naples, FL) were used as retrograde tracers. The CTB-AlexaFluor 488 conjugate appears green under the fluorescein isothiocyanate (FITC) filter and will be referred to as *CTB-green*. The CTB-AlexaFluor 594 conjugate appears red under the Texas red filter and will be referred to as *CTB-red*. The red and green latex microspheres fluoresce under rhodamine and FITC filters, respectively. In five of the cases in which the CTB conjugates were used (*rVA-1-3* and *rH45-1* and *-2*) the solution was iontophoretically injected (+4 μ A, 7 seconds on/7 seconds off) for 30 minutes. Immediately prior to the injection, the CSA was recorded again with the injection pipette to verify the cell type. In cases *rVA-4*, *rH45-3*, and *rH45-4*, the tracers were pressure injected with a Picospritzer II (General Valve Corporation; 40 psi, 100 msec duration/puff). After injection, the electrode was undisturbed for 5–10 minutes. After surgery, the craniotomy was filled with bone wax and the wound sutured. Birds were given an intramuscular injection of buprenorphine (0.012 mg/kg) as an analgesic.

After a recovery period of 2–5 days, the animals were deeply anesthetized with sodium pentobarbital (100 mg/kg) and immediately perfused with heparinized phosphate-buffered saline (PBS; 0.9% NaCl, 1 ml/100 ml heparin, 0.1 M phosphate buffer). The brains were extracted and then flash frozen in 2-methylbutane and stored at -80°C until sectioning. Brains were embedded in optimal cutting temperature medium and 25–40 μ m coronal sections were cut through the brainstem and cerebellum with a cryostat and mounted on electrostatic slides.

With the exception of case *rH45-4*, two series were collected. One series was coverslipped with geltol and examined via fluorescence microscopy (fluorescence series). For the second series, a chromagen was used to visualize the CTB with immunohistochemistry for examination via light microscopy (chromagen series). (In some cases the chromagen series was first examined for fluorescence.) These mounted sections were fixed in 10% formalin and put through ethanol washes and xylene to dehydrate, defat, and rehydrate. Sections were then rinsed with 0.1 M PBS, pH 7.4, and double-distilled water, washed with 1% H_2O_2 in 50% MeOH for 10 minutes to remove endogenous peroxidases, then rinsed in PBS and double-distilled water. Sections were blocked with 10% rabbit serum + 0.4% Triton X-100 in PBS for 30 minutes at room temperature, then incubated in goat anticholeragenoid

(CTB subunit) with 0.4% Triton X-100 (703; List Biological, Campbell, CA; 1:10,000) in PBS for 20 hours at 4°C . Sections were then rinsed with PBS and incubated with biotinylated rabbit anti-goat antiserum with 0.4% Triton X-100 (RAG; BA-5000; Vector, Burlingame, CA; 1:300) in PBS for 60 minutes. After rinsing with PBS, either avidin biotin complex (1:100) was added for 30 minutes at room temperature or ExtrAvidin (Sigma, St. Louis, MO; 1:1,000) and 0.4% Triton X-100 in PBS for 90 minutes at room temperature. Sections were then stained with metal-enhanced 3,3'-diaminobenzidine tetrahydrochloride tablets (DAB; Sigma) for 1–5 minutes.

Sections were viewed with a compound light microscope (Olympus Research Microscope BX60) equipped with the appropriate fluorescence filters (Texas red and FITC filters for the CTB-AlexaFluor, rhodamine and FITC for the latex microspheres). Images were obtained with a digital camera (Media Cybernetics CoolSnap-Pro color digital camera) and Adobe Photoshop software was used to compensate for brightness and contrast.

Nomenclature: rostral vs. caudal mcIO

The pigeon IO has been divided into ventral and dorsal lamella, which are conjoined medially by the mcIO (Arends and Voogd, 1989). Throughout the text, we refer to the olivary input to the *rVA* and *rH45* zones as originating in the rostral and caudal mcIO, respectively. The rostrocaudal extent of the mcIO ranges from about 1.5 to 1.8 mm. In our previous work (Wylie et al., 1999), we showed that retrograde labeling from injections into the *rVA* zones is concentrated in the caudal 700–800 μ m, whereas labeling from *rH45* zones is concentrated in the rostral 700–800 μ m. The border between those areas projecting to the *rVA* and *rH45* zones could be quite sharp (see Fig. 1 of Wylie et al., 1999), but there is probably some overlap (see Table 1 of Wylie et al., 1999). Thus, our distinction of caudal and rostral mcIO should not be taken as an absolute but is comparable to the distinction between caudal and rostral dorsal cap in rabbits and rats (Alley et al., 1975; Ruigrok et al., 1992; Tan et al., 1995b).

RESULTS

Experiments were performed on eight pigeons. In cases *rVA-1-3*, the pigeons received iontophoretic injections of the CTB-Alexafluor conjugate, one injection in the caudomedial *rVA* zone (zone 0) and one injection in the rostrolateral *rVA* zone (zone 2). In case *rVA-4*, pressure injections of the CTB-Alexafluor conjugates were made, CTB-green in zone 2 and CTB-red in zone 0. In cases *rH45-1* and *-2*, iontophoretic injections of the CTB-Alexafluor conjugate were made, one injection into the caudomedial *rH45* zone (zone 1) and the other injection into the rostrolateral *rH45* zone (zone 3). In case *rH45-4*, pressure injections of latex microspheres were made, green beads into zone 3 and red beads into zone 1.

Figure 2A–C shows data from case *rVA-1*. Figure 2B shows the injection site in the dorsal lamella of folium IXcd in zone 0. The center of the injection was 2.7 mm from the midline. From a section 1.43 mm rostral to that shown in Figure 2B, Figure 2C shows the injection site in zone 2, medially in the caudal part of the auricle (Au). The center of this injection was 3.3 mm from the midline. Figure 2A is a series of drawings of coronal sections through the IO, from the chromagen series, showing the

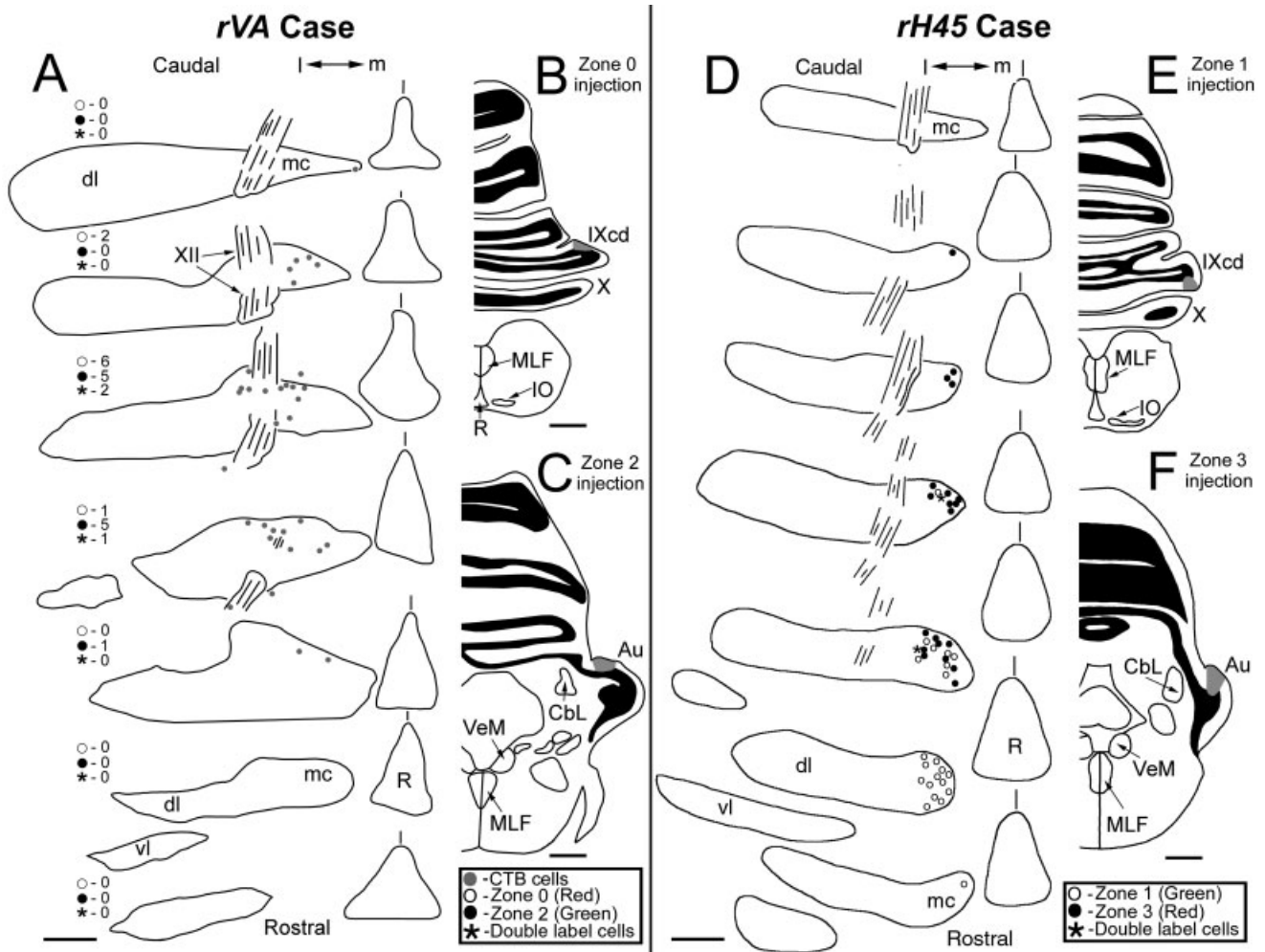


Fig. 2. Projections from the medial column of the inferior olive (mcIO) to the *rVA* and *rH45* zones of the pigeon flocculus. **A–C** show data from experiment *rVA*-1. **A** shows camera lucida drawings of coronal sections through the mcIO, 190 μm apart, from caudally to rostrally. **B** and **C** show drawings of the injection sites (gray regions) in zones 0 and 2, respectively. The sections from **A** were taken from the series processed for CTB immunocytochemistry, and the gray circles indicate the location of CTB-labeled cells. On each drawing, the number of single-labeled cells from zones 0 (open circles) and 2 (solid

circles) and the number of double-labeled cells (asterisks) observed in the adjacent sections are also indicated. **D–F** show data from *rH45*-2. **D** shows drawings of coronal sections through the mcIO at 160- μm intervals. **E** and **F** show drawings of the injections in zones 1 and 3, respectively. In **D**, locations of single-labeled cells from the injections in zones 1 (open circles) and 3 (solid circles) as well as double-labeled cells (asterisks) are shown. See list for abbreviations. See text for details. Scale bars = 200 μm in **A**, **D**; 1 mm in **B**, **C**, **E**, **F**.

location of retrogradely labeled cells (gray circles) in the contralateral mcIO from these injections. Those neurons labeled from the zone 0 and zone 2 injections are indistinguishable in the chromagen series. However, the numbers of labeled cells from zone 0 (open circles), zone 2 (solid circles), and double labeled cells (asterisks) are listed for the adjacent (caudal) sections from the fluorescence series. The retrograde labeling was concentrated in the caudal 700–800 μm of the contralateral mcIO, consistent with our previous findings (Wylie et al., 1999). Also, there was a slight difference in the rostrocaudal distribution of cells labeled from the zone 0 and zone 2 injections (addressed in detail below; see Fig. 4).

Figure 2D–F shows data from case *rH45*-2. Figure 2E shows the injection site in the ventral lamella of IXcd in zone 1. The center of the injection was 3.4 mm from the

midline. From a section 1.44 mm rostral to that shown in Figure 2E, Figure 2F shows the injection site in zone 3, in the rostral Au. The center of this injection was 4.4 mm from the midline. Figure 2D is a series of drawings of coronal sections through the IO, from the chromagen series, showing the location of retrogradely labeled cells in the contralateral mcIO. These sections were first examined for fluorescence; thus, we were able to assign cells as either single labeled from zone 1 (open circles) or zone 3 (solid circles) or double labeled (asterisks). Consistent with our previous findings (Wylie et al., 1999), the retrograde labeling was concentrated in the rostral 700–800 μm of the contralateral mcIO. Also, there was a difference in the rostrocaudal distribution of cells labeled from the zone 1 and zone 3 injections (addressed in detail below; see Fig. 4).

TABLE 1. Number of Retrogradely Labeled Cells in the Medial Column of the Inferior Olive (mcIO) from Each Injection¹

Case	Zone 0	Zone 2	Double labeled (%)	Case	Zone 1	Zone 3	Double labeled (%)
<i>rVA-1</i>	17	28	6 (35)	<i>rH45-1</i>	25	88	4 (16)
<i>rVA-2</i>	81	56	9 (16)	<i>rH45-2</i>	95	80	5 (6)
<i>rVA-3</i>	45	11	1 (9)	<i>rH45-3</i>	289	314	68 (24)
<i>rVA-4</i>	158	303	44 (28)	<i>rH45-4</i>	29	389	7 (24)
Mean			(22)				(18)

¹In all *rVA* cases, the labeling was restricted to the caudal half of the mcIO. In cases *rH45-1* and 2, the labeling was restricted to the rostral half of the mcIO. In cases *rH45-3* and 4, there was some labeling in the caudal half of the mcIO. However, only the cells in the rostral mcIO were tabulated below for these cases.

The fact that the labeling was concentrated in the caudal mcIO from the *rVA* injections, and the rostral mcIO from the *rH45* injections, indicates that the injections were predominantly in a single zone and encroached minimally upon adjacent zones. The injection sites resulting from iontophoresis were typically small, ranging in diameter from 190–300 μm . The number of olivary cells labeled from each of the iontophoretic injections varied from 11 to 95 (mean = 52.6; see Table 1). In the cases involving pressure injections (*rVA-4*, *rH45-3*, *rH45-4*), the injections were larger, ranging in diameter from 300 to 500 μm . Also, the number of retrogradely labeled cells from each injection was generally larger (33–482; mean = 266.8) compared with the iontophoretic injections. In case *rVA-4*, the retrogradely labeled cells were confined to the caudal mcIO, again indicating that the injections encroach minimally upon the adjacent zones. In cases *rH45-3* and *rH45-4*, although the bulk of the retrograde labeling was in the rostral mcIO, some was found in the caudal mcIO. In case *rH45-3*, from the zone 1 injection, 289 cells were found in the rostral mcIO, but two (<1%) were observed in the caudal mcIO. This indicates that the spread to the adjacent zones 0 and/or zone 2 was negligible. From the zone 3 injection, 314 cells were found in the rostral mcIO, and 20 (6%) were found in the caudal mcIO. Again, this indicates that the spread to the adjacent zone 2 was minimal. In case *rH45-4*, from the zone 1 injection, 29 cells were found in the rostral mcIO, and four (12%) were observed in the caudal mcIO. From the injection in zone 3 (also from case *rH45-4*), the largest of all injections, 389 cells were found in the rostral mcIO, and 93 (19%) were found in the caudal mcIO. Clearly, this injection spread into the adjacent *rVA* zone 2 and, possibly, as far as zone 1. However, examination of the sections by fluorescent microscopy showed that the CTB-red and CTB-green injections did not overlap.

Figure 3 shows a montage of photomicrographs. Typical retrograde labeling from four different sections is shown in Figure 3A–L. Figure 3A–C is from a section in the rostral mcIO from case *rH45-3*. Figure 3A shows two cells labeled with CTB-green from an injection in zone 1. Figure 3B shows that these cells were also labeled with CTB-red from an injection in zone 3, plus an additional cell that was not double labeled. Figure 3C is from the same section in which the CTB was visualized with immunohistochemistry. The three labeled cells can be seen clearly. In those sections that we examined first with fluorescence and then subsequently processed for immunohistochemistry, the concordance was virtually 100%. Figure 3D–F is from a section obtained through the caudal mcIO from case *rVA-4*. Figure 3D shows seven cells labeled with CTB-green from a pressure injection in zone 2. Figure 3E shows six cells labeled with CTB-red from a pressure injection in zone 0.

Figure 3F shows the same section; the green and red images have been overlaid, and three double labeled cells can be seen. Figure 3G–I is from a section in the caudal mcIO from case *rVA-2*. Figure 3G shows two cells labeled with CTB-green from an iontophoretic injection in zone 2. Figure 3H shows two cells labeled with CTB-red from an iontophoretic injection in zone 0. Figure 3I shows an overlaid image of the green and red frames and a double labeled cell intermingled with the green and red cells. Figure 3J–L shows labeled cells in the rostral mcIO from *rH45-4*. Figure 3J shows numerous labeled cells from a pressure injection of green latex microspheres in zone 3. Figure 3K shows four labeled cells resulting from a pressure injection of red latex microspheres into zone 1. Figure 3L shows the overlay of the green and red images; one cell was double labeled.

The total number of labeled cells and percentage of double labeled cells from each case are shown in Table 1. The percentage of double labeled cells for each case was expressed as a ratio between the number of double labeled cells and the total number of labeled cells from the zone with the smaller cell count. The percentages of double labeled cells averaged 22% for the *rVA* cases and 18% for the *rH45* cases.

From the photomicrographs in Figure 3, it is apparent that the red and green cells were intermingled in a given section. However, a close inspection of the data revealed a slight rostrocaudal difference in the distribution of cells in the mcIO labeled from the two *rVA* zones and the two *rH45* zones. This observation is illustrated by the histograms in Figure 4. With respect to the *rVA* zones, the distribution of cells labeled from zone 0 was slightly caudal to that from zone 2. The opposite pattern was seen with the *rH45* zones; the distribution of cells labeled from zone 1 was slightly rostral to that from zone 3. Figure 4A shows the distribution of olivary cells retrogradely labeled from zone 0 (white bars) and zone 2 (black bars) injections. To obtain these data, the rostrocaudal extent of the IO was organized in 100 μm bins from the caudal tip of the mcIO. The number of labeled cells in each 100 μm bin from each injection was converted into a percentage of the total number of labeled cells from that injection for each case. Subsequently, all four *rVA* cases were averaged. Similarly, Figure 4B shows the distribution of olivary cells retrogradely labeled from zone 1 (white bars) and zone 3 (black bars) injections. This histogram was created as described for the *rVA* cases, except the bins were calculated beginning from the rostral tip of the mcIO. The cells found in the caudal half of the mcIO from cases *rH45-3* and *rH45-4* (see above) were not included in the analysis. From Figure 4A, it appears that there is a slight rostrocaudal difference in the distributions of cells projecting to the different *rVA* zones. Although the distributions are

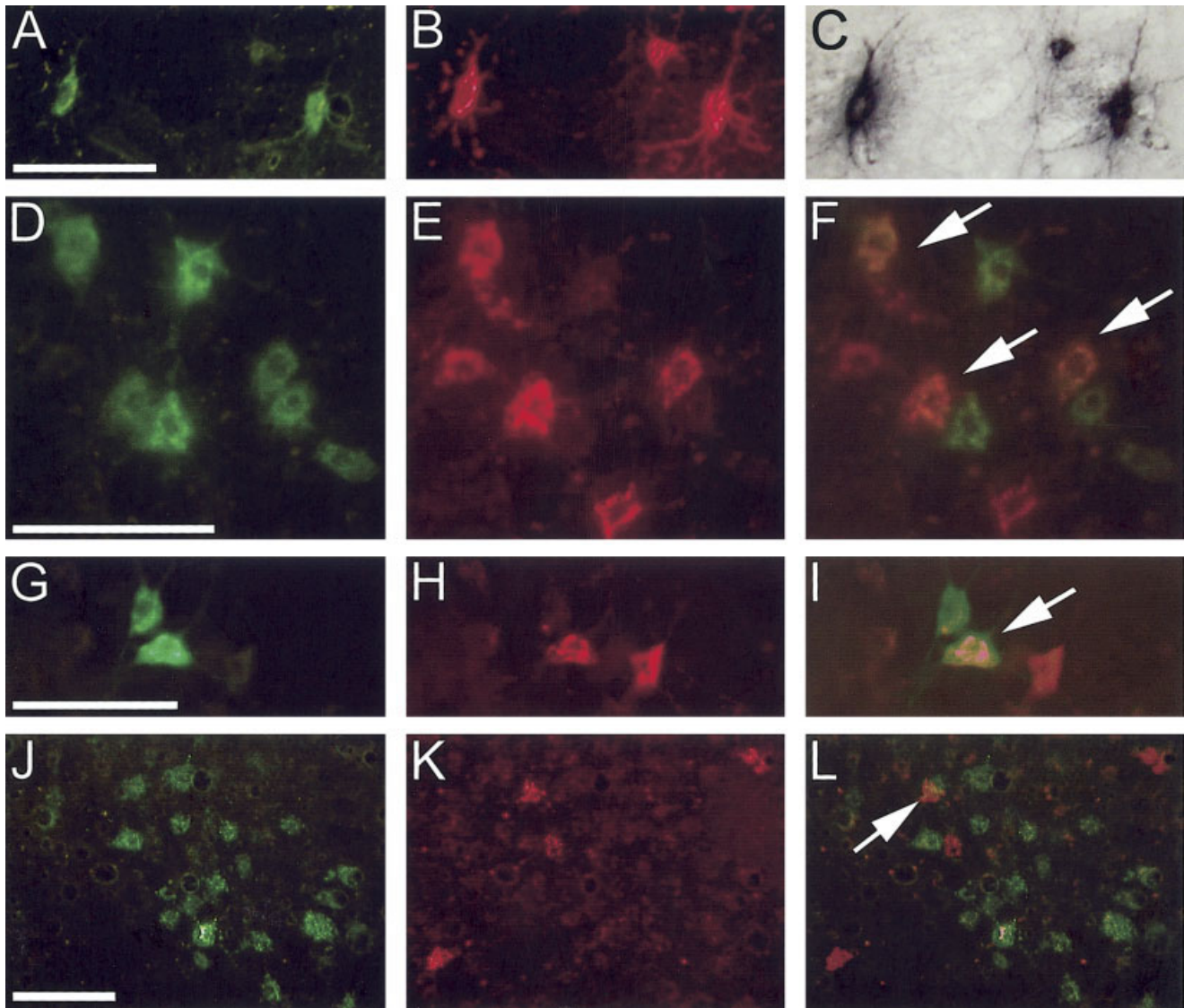


Fig. 3. **A–L** show retrogradely labeled cells in the medial column of the inferior olive (mcIO). Data from four different sections are shown, in triplets (**A–C**, **D–F**, **G–I**, **J–L**). **A**, **D**, and **G** show cells labeled with CTB-green. **B**, **E**, and **H** show cells labeled with CTB-red. **J** and **K** show cells labeled with green and red latex microspheres, respec-

tively. **C** shows the section when labeled cells are visualized with DAB. **F**, **I**, and **L** show the overlay of the corresponding green and red sections. Arrows indicate double-labeled cells in overlaid pictures. For details, see text. Scale bars = 100 μm in **A** (applies to **A–C**), **D** (applies to **D–F**), **G** (applies to **G–I**), **J** (applies to **J–L**).

by-and-large overlapping, that from zone 0 is slightly caudal to that from zone 2. From Figure 4B, there appears to be a comparatively larger rostrocaudal difference in the distributions of cells projecting to the different *rH45* zones; that from zone 1 is rostral to that from zone 3. We tested for differences between the rostrocaudal distributions of the *rVA* zones and the *rH45* zones by using two statistical tests. First, we compared distributions of cell counts between the two injection sites (i.e., either zone 0 and zone 2 for the *rVA* cases or zone 1 and zone 3 for the *rH45* cases) by using a categorical Kolmogorov-Smirnov test of independence (Zar, 1999). [Typical tests of independence, such as the χ^2 test, are not appropriate, because the categories (i.e., the bins) are ordinal.] Significance levels were calculated by comparing the empirical Kolmogorov-

Smirnov test statistic against a distribution of test statistics calculated from 1,000 randomizations of the same data under the null hypothesis (that the data are distributed in proportion to their expected frequencies in a test of independence). The distribution of cells labeled from the zone 1 injections was significantly different from that labeled from the zone 3 injections in all four *rH45* cases, and the distribution of cells labeled from the zone 0 injections was significantly different from that labeled from the zone 2 injections in three of the four *rVA* cases (see Appendix A). Second, we also tested to see whether the two injection sites labeled cells in more rostral vs. caudal sections using a Welch's *t*-test (see Appendix B). All four *rH45* cases showed significantly more cells in the rostral most sections of the mcIO from the zone 1 injection compared with

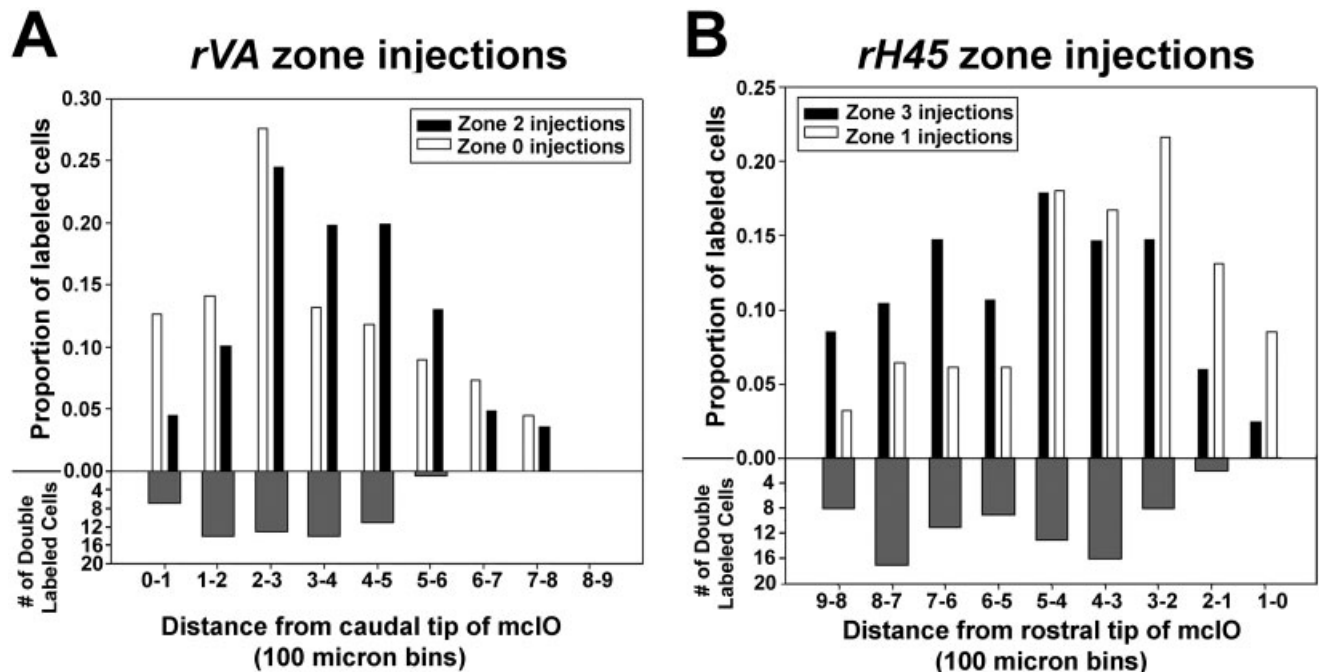


Fig. 4. Histograms illustrating a slight rostrocaudal difference in the distribution of cells labeled from the two *rVA* zones (A) and the two *rH45* zones (B). In A, the rostrocaudal extent of the inferior olive (IO) is organized in 100- μ m bins starting from the caudal tip of the medial column of the inferior olive (mcIO). In B, the rostrocaudal extent of the IO is organized in 100- μ m bins beginning from the

rostral tip of the mcIO. The distribution of olivary cells retrogradely labeled is illustrated from injections in zones 0 and 1 (white bars) and zones 2 and 3 (black bars). The lower histograms show the total number of double-labeled cells in each bin from all four cases. See text for details.

the zone 3 injection. Two of the four *rVA* cases showed significantly more labeled cells in the caudalmost sections of the mcIO from the zone 0 injection compared with the zone 2 injection. In summary, from these two statistical tests, there was unambiguous support for the assertion that the distribution of cells labeled from the zone 1 injection was rostral to that from the zone 3 injection, and there was strong support for the assertion that the distribution of cells labeled from the zone 0 injection was caudal to that from the zone 2 injection.

In Figure 4A,B we also show the rostrocaudal distribution of double labeled cells from the *rVA* and *rH45* cases. This is illustrated in the lower histograms, which indicate the number of double labeled cells in each bin totaled from all four cases. The distribution of double labeled cells in the mcIO is unremarkable insofar as the double labeled cells were not found in any particular location among the single labeled neurons.

DISCUSSION

Olivary projection to the floccular zones in mammals and birds

It has been shown in several species that the flocculus is compartmentalized such that there are multiple *rVA* zones interleaved with multiple *rH45* zones (for review see Voogd and Wylie, 2004). Physiological and anatomical studies in rabbits have shown that there are in total four visual zones in the flocculus. Zones 1 and 3 are *rH45* zones that receive input from the rostral dorsal cap (DC) and

ventrolateral outgrowth (VLO), whereas zones 2 and 4 are *rVA* zones that receive input from the caudal DC (Alley et al., 1975; Leonard et al., 1988; De Zeeuw et al., 1994; van der Steen et al., 1994; Tan et al., 1995b; see also Yamamoto and Shimoyama, 1977; Yamamoto, 1978; Sato and Kawasaki, 1991). Insofar as they provide input to *rH45* zones, the VLO and rostral DC in rabbits correspond to the rostral mcIO in pigeons. Likewise, insofar as they provide input to *rVA* zones, the caudal DC corresponds to the caudal mcIO in pigeons (Wylie et al., 1999, 2003; Winship and Wylie, 2001, 2003). Comparable electrophysiological studies have not been performed with rats, but neuroanatomical studies have shown that there are three zones innervated by the DC (zones 0, 2, and 4) interdigitated with two zones receiving input from the VLO (zones 1 and 3; Sugihara et al., 2004; see also Ruigrok et al., 1992; Balaban et al., 2000; Ruigrok, 2003). Although the physiological work has not been performed, we believe it likely that zones 0, 2, and 4 are *rVA* zones and zones 1 and 3 are *rH45* zones (Voogd and Wylie, 2004). The zonal nomenclature that we used for the pigeon floccular zones in the present paper, outlined in Figure 1, was adopted to provided the most logical correspondence with the zones in the rabbit and rat. Zone 0, not present in rabbits, is the most lateral visual zone in the rat flocculus but corresponds to the most medial *rVA* zone in pigeons. This is because the part of the mammalian cerebellum that contains the flocculus folds back on itself and twists (Bolk, 1906) such that the order of zones becomes reversed in a

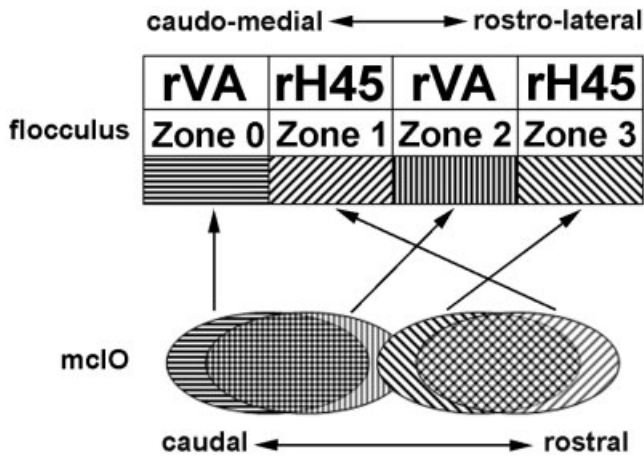


Fig. 5. Diagram of the projections from the medial column of the inferior olive (mcIO) to the zones of the flocculus. Overlapping patterns indicate overlapping distribution of olivofloccular projections.

coronal section. There is also a nonvisual zone in the rabbit flocculus, zone C2, which has been linked to head movement (De Zeeuw et al., 1994; Tan et al., 1995a; De Zeeuw and Koekkoek, 1997).

There are also zones in the nodulus and ventral uvula of rats and rabbits that are innervated by the DC and VLO (Balaban and Henry, 1988; Katayama and Nisimaru, 1988; Voogd et al., 1996; Ruigrok, 2003). Electrophysiological studies in rabbits have confirmed that there are alternating *rVA* and *rH45* zones (Kano et al., 1990; Barmack and Shojaku, 1992; Wylie et al., 1994). This is not the case in pigeons. In pigeons, CSA in the nodulus and ventral uvula is modulated by optic flow patterns resulting from self-translation (Wylie and Frost, 1991, 1999; Wylie et al., 1993, 1998), and the olivary input arises from regions immediately lateral to those areas projecting to the flocculus (Lau et al., 1998; Wylie et al., 1999; Crowder et al., 2000).

In the present study we found that, with respect to the projection of the caudal mcIO, there was a differential projection to zones 0 and 2. Although by-and-large overlapping, the distribution of cells retrogradely labeled from zone 0 was slightly caudal to that of cells labeled from zone 2. Similarly, with respect to the projection of the rostral mcIO, there was a differential projection to zones 1 and 3. The distribution of cells retrogradely labeled from zone 1 was slightly rostral to that from zone 3. This aspect of the olivary projection to the flocculus is illustrated in Figure 5. Although it was not reported as such, it appears that Sugihara et al. (2004) might have revealed a similar pattern with respect to the VLO projection to zones 1 and 3 in rats. They reconstructed single olivocerebellar axons labeled with the anterograde tracer biotinylated dextran. All of the axons originating from cells in the rostral VLO projected to zone 1, whereas two of the five axons originating from cells in the caudal VLO projected to zone 3. These findings suggest that there may be a rostral-caudal difference with respect to the projection from the VLO to zones 1 and 3, similar to what we found in the present study.

Climbing fibers innervating multiple zones

Generally, a CF axon will innervate a single zone or even a single microzone (Sugihara et al., 1999, 2001, 2003). However, it has been shown that some CFs in the olivovestibulocerebellar system innervate multiple zones. For example, by using electrophysiological and double retrograde techniques, Takeda and Maekawa (1989a,b) showed that some olivary neurons innervate both the flocculus and the vermal vestibulocerebellum (nodulus and uvula) in rabbits. Similarly, Ruigrok (2003) showed, based on cortical injections into the flocculus or nodulus in rats, that some olivary neurons in the DC innervate *rVA* zones in both the nodulus and the flocculus, and some VLO neurons innervate *rH45* zones in both the nodulus and the flocculus. Sugihara et al. (2004) also reconstructed one DC neuron that innervated zone 2 of the flocculus and the lateral *rVA* zone in the nodulus and one VLO neuron that innervated zone 1 of the flocculus and the *rH45* zone of the nodulus. They also noted that some DC and VLO neurons innervated the flocculus and the anterior vermis (see also Ruigrok, 2003). Ruigrok (2003) as well noted that some DC neurons innervated the medial and lateral *rVA* zones in the nodulus in rats.

Most pertinently to the present study, both Sugihara et al. (2004) and Ruigrok (2003) found that individual CFs innervate multiple floccular zones in rats. From an injection of CTB into zone 1, collateral labeling of CFs was found in zones 1 and 3 (Ruigrok, 2003). Sugihara et al. (2004) reconstructed the axons of 24 CFs originating in the DC or VLO. One CF innervated more than one floccular zone (zones 2 and 4), although some (six) of these CFs innervated a floccular zone as well as the nodulus or the anterior vermis. In the present study, we found that 20% of mcIO neurons projected to more than one zone in the pigeon flocculus, although this was quite variable among cases (6–35%). We consider 20% to be an underestimate in this regard. To obtain an accurate and complete account of the percentage of cells projecting to multiple zones, one would have to inject an entire zone to its boundaries. However, to have some assurance that the injections were confined to a single zone, small injections were desired. It is worth noting that the two largest injections (cases *rVA*-4, *rH45*-3) had a higher percentage of double-labeled neurons (average = 25%).

The phenomenon of single olivary neurons innervating multiple zones is not to be limited to the vestibulocerebellum. For example, in the vermis, the rostral compartments of zones X and CX both receive input from the b and c subnuclei of the medial accessory olive (Buisseret-Delmas et al., 1993). In the anterior lobe, zones C1, C3, and Y all receive input from rostral dorsal accessory olive (Groenewegen et al., 1979; Trott and Apps, 1993; Garwicz et al., 1998). It has been shown that single olivary neurons innervate multiple zones in this system (Ekerot and Larson, 1982). After injections of different colors of fluorescent tracers into the C1 and C3 zones, Apps and Garwicz (2000) found that different but overlapping regions of the rDAO were labeled. They found that on average 16.5% of the neurons were double labeled. In this respect, these findings are remarkably similar to those in the present study. Apps and Garwicz (2000) also coinjected fluorescent retrograde and anterograde tracers into the C1 and C3 regions and found that there was a tight correspondence between the overlap of the corticonuclear projec-

tions and the amount of overlap and double labeling in the inferior olive. These results emphasize that the functional unit of the olivocerebellar system is the module consisting of multiple cortical zones (or microzones), its divergent olivary input, and its convergent corticonuclear output (Voogd and Bigare, 1980; Apps and Garwicz, 2000; Bukowska et al., 2002). Further elucidation of the details of the underlying connectivity of the cerebellar modules is critical to our understanding of how the cerebellum is involved in motor control and other processes (Ito, 1984; Garwicz et al., 1998).

LITERATURE CITED

- Alley K, Baker R, Simpson JI. 1975. Afferents to the vestibulocerebellum and the origin of the visual climbing fibers in the rabbit. *Brain Res* 98:582–589.
- Apps R, Garwicz M. 2000. Precise matching of olivo-cortical divergence and cortico-nuclear convergence between somatotopically corresponding areas in the medial C1 and medial C3 zones of the paravermal cerebellum. *Eur J Neurosci* 12:205–214.
- Arends JJA, Voogd J. 1989. Topographic aspects of the olivocerebellar system in the pigeon. *Exp Brain Res* 17(Suppl):52–57.
- Balaban CD. 1988. Distribution of inferior olivary projections to the vestibular nuclei of albino rabbits. *Neuroscience* 24:119–134.
- Balaban CD, Schuerger RJ, Porter JD. 2000. Zonal organization of flocculo-vestibular connections in rats. *Neuroscience* 99:669–682.
- Barmack NH, Shojaku H. 1992. Vestibularly induced slow oscillations in climbing fiber responses of Purkinje cells in the cerebellar nodulus of the rabbit. *Neuroscience* 50:1–5.
- Bolk L. 1906. *Das Cerebellum der Säugetiere*. Jena: Fischer.
- Buisseret-Delmas C, Yatim N, Buisseret P, Angaut P. 1993. The X zone and CX subzone of the cerebellum in the rat. *Neurosci Res* 16:195–207.
- Bukowska D, Zguczynski L, Mierzejewska-Krzyzowska B. 2002. Axonal collateral branching of neurones in the inferior olive projecting to the cerebellar paramedian lobule in the rabbit. *Cell Tissue Res* 172:37–47.
- Crowder NA, Winship IR, Wylie DR. 2000. Topographic organization of inferior olive cells projecting to translational zones in the vestibulocerebellum of pigeons. *J Comp Neurol* 419:87–95.
- De Zeeuw CI, Koekkoek SK. 1997. Signal processing in the C2 module of the flocculus and its role in head movement control. *Prog Brain Res* 114:299–320.
- De Zeeuw CI, Wylie DR, DiGiorgi PL, Simpson JI. 1994. Projections of individual Purkinje cells of identified zones in the flocculus to the vestibular and the cerebellar nuclei in the rabbit. *J Comp Neurol* 349:428–447.
- Ekerot C-F, Larson B. 1982. Branching of olivary axons to innervate pairs of sagittal zones in the cerebellar anterior lobe of the cat. *Exp Brain Res* 48:185–198.
- Ezure K, Graf W. 1984. A quantitative analysis of the spatial organization of the vestibulo-ocular reflexes in lateral and frontal-eyed animals. I. Orientation of semicircular canals and extraocular muscles. *Neuroscience* 12:85–93.
- Garwicz M, Ekerot C-F, Jorntell H. 1998. Organizational principles of cerebellar neuronal circuitry. *New Physiol Sci* 13:26–32.
- Graf W, Simpson JI, Leonard CS. 1988. Spatial organization of visual messages of the rabbit's cerebellar flocculus. II. Complex and simple spike responses of Purkinje cells. *J Neurophysiol* 60:2091–2121.
- Groenewegen HJ, Voogd J, Freedman SL. 1979. The parasagittal zonation with the olivocerebellar projection. II. Climbing fibre distribution in the intermediate and hemispheric parts of the cerebellum. *J Comp Neurol* 183:551–602.
- Ito M. 1984. *The cerebellum and neural control*. New York: Raven.
- Kano M, Kano MS, Kusunoki M, Maekawa K. 1990. Nature of optokinetic response and zonal organization of climbing fiber afferents in the vestibulocerebellum of the pigmented rabbit. II. The nodulus. *Exp Brain Res* 80:238–251.
- Karten HJ, Hodon W. 1967. *A stereotaxic atlas of the brain of the pigeon (Columba livia)*. Baltimore: Johns Hopkins Press.
- Katayama S, Nisimaru N. 1988. Parasagittal zonal pattern of olivonodular projections in rabbit cerebellum. *Neurosci Res* 5:424–438.
- Lau KL, Glover RG, Linkenhoker B, Wylie DR. 1998. Topographical organization of inferior olive cells projecting to translation and rotation zones in the vestibulocerebellum of pigeons. *Neuroscience* 85:605–614.
- Leonard CS, Simpson JI, Graf W. 1988. Spatial organization of visual messages of the rabbit's cerebellar flocculus. I. Typology of inferior olive neurons of the dorsal cap of Kooy. *J Neurophysiol* 60:2073–2090.
- Ruigrok TJ. 2003. Collateralization of climbing and mossy fibers projecting to the nodulus and flocculus of the rat cerebellum. *J Comp Neurol* 466:278–298.
- Ruigrok TJH, Osse RJ, Voogd J. 1992. Organization of inferior olivary projections to the flocculus and ventral paraflocculus of the rat cerebellum. *J Comp Neurol* 316:129–150.
- Sato Y, Kawasaki T. 1991. Identification of Purkinje cell/climbing fiber zone and its target neurons responsible for eye-movement control by the cerebellar flocculus. *Brain Res Rev* 16:39–64.
- Simpson JI, Graf W. 1981. Eye-muscle geometry and compensatory eye movements in lateral-eyed and frontal-eyed animals. *Ann N Y Acad Sci* 374:20–30.
- Simpson JI, Graf W. 1985. The selection of reference frames by nature and its investigators. In: Berthoz A, Melvill-Jones G, editors. *Adaptive mechanisms in gaze control: facts and theories*. Amsterdam: Elsevier. p 3–16.
- Simpson JI, Graf W, Leonard C. 1981. The coordinate system of visual climbing fibres to the flocculus. In: Fuchs AF, Becker W, editors. *Progress in oculomotor research*. Amsterdam: Elsevier North Holland.
- Simpson JI, Leonard CS, Soodak RE. 1988a. The accessory optic system: analyzer of self-motion. *Ann N Y Acad Sci* 545:170–179.
- Simpson JI, Leonard CS, Soodak RE. 1988b. The accessory optic system: II. Spatial organization of direction selectivity. *J Neurophysiol* 60:2055–2072.
- Simpson JI, Graf W, Leonard CS. 1989a. Three-dimensional representation of retinal image movement by climbing fiber activity. In: Strata P, editor. *The olivocerebellar system in motor control: experimental brain research supplement*, vol 17. Heidelberg: Springer-Verlag. p 323–327.
- Simpson JI, Van der Steen J, Tan J, Graf W, Leonard CS. 1989b. Representations of ocular rotations in the cerebellar flocculus of the rabbit. *Prog Brain Res* 80:213–223.
- Sugihara I, Wu H-S, Shinoda Y. 1999. Morphology of single olivocerebellar axons labeled with biotinylated dextran amine in the rat. *J Comp Neurol* 414:131–148.
- Sugihara I, Wu H-S, Shinoda Y. 2001. The entire trajectories of single olivocerebellar axons in the cerebellar cortex and their contribution to cerebellar compartmentalization. *J Neurosci* 21:7715–7723.
- Sugihara I, Lohof AM, Letellier M, Mariani J, Sherrard RM. 2003. Postlesion transcommissural growth of olivary climbing fibres creates functional synaptic microzones. *Eur J Neurosci* 18:3027–3036.
- Sugihara I, Ebata S, Shinoda Y. 2004. Functional compartmentalization in the flocculus and the ventral dentate and dorsal group y nuclei: an analysis of single olivocerebellar axonal morphology. *J Comp Neurol* 470:113–133.
- Takeda T, Maekawa K. 1989a. Olivary branching projections to the flocculus, nodulus and uvula in the rabbit. I. An electrophysiological study. *Exp Brain Res* 74:47–62.
- Takeda T, Maekawa K. 1989b. Olivary branching projections to the flocculus, nodulus and uvula in the rabbit. II. Retrograde double labeling study with fluorescent dyes. *Exp Brain Res* 76:323–332.
- Tan J, Simpson JI, Voogd J. 1995a. Anatomical compartments in the white matter of the rabbit flocculus. *J Comp Neurol* 356:51–71.
- Tan J, Gerrits NM, Nanhoe JI, Simpson JI, Voogd J. 1995b. Zonal organization of the climbing fiber projection to the flocculus and nodulus of the rabbit: a combined axonal tracing and acetylcholinesterase histochemical study. *J Comp Neurol* 356:23–50.
- Trott JR, Apps R. 1993. Zonal organization within the projection from the inferior olive to the rostral paramedian lobule of the cat cerebellum. *Eur J Neurosci* 5:162–173.
- van der Steen J, Simpson JI, Tan J. 1994. Functional and anatomic organization of three-dimensional eye movements in rabbit cerebellar flocculus. *J Neurophysiol* 72:31–46.
- Voogd J, Bigare F. 1980. Topographical distribution of olivary and corticonuclear fibers in the cerebellum: a review. In: Courville J, de Montigny C, Lamarre Y, editors. *The inferior olivary nucleus*. New York: Raven. p 207–234.
- Voogd J, Wylie DR. 2004. Functional and anatomical organization of flocc-

- cular zones: a preserved feature in vertebrates. *J Comp Neurol* 470: 107–112.
- Voogd J, Gerrits NM, Ruigrok TJ. 1996. Organization of the vestibulocerebellum. *Ann N Y Acad Sci* 781:553–579.
- Winship IR, Wylie DRW. 2001. Responses of neurons in the medial column of the inferior olive in pigeons to translational and rotational optic flowfields. *Exp Brain Res* 141:63–78.
- Winship IR, Wylie DRW. 2003. Zonal organization of the vestibulocerebellum in pigeons (*Columba livia*): I. Climbing fibre input to the flocculus. *J Comp Neurol* 456:127–139.
- Wylie DR, Frost BJ. 1991. Purkinje cells in the vestibulocerebellum of the pigeon respond best to either rotational or translational visual flow. *Exp Brain Res* 86:229–232.
- Wylie DR, Frost BJ. 1993. Responses of pigeon vestibulocerebellar neurons to optokinetic stimulation. II. The 3-dimensional reference frame of rotation neurons in the flocculus. *J Neurophysiol* 70:2647–2659.
- Wylie DR, Frost BJ. 1996. The pigeon optokinetic system: visual input in extraocular muscle coordinates. *Vis Neurosci* 13:945–953.
- Wylie DR, Frost BJ. 1999. Responses of neurons in the nucleus of the basal optic root to translational and rotational flowfields. *J Neurophysiol* 81:267–276.
- Wylie DR, Kripalani T, Frost BJ. 1993. Responses of pigeon vestibulocerebellar neurons to optokinetic stimulation. I. Functional organization of neurons discriminating between translational and rotational visual flow. *J Neurophysiol* 70:2632–2646.
- Wylie DR, De Zeeuw CI, DiGiorgi PL, Simpson JI. 1994. Projections of individual Purkinje cells of physiologically identified zones in the ventral nodulus to the vestibular and cerebellar nuclei in the rabbit. *J Comp Neurol* 349:448–463.
- Wylie DR, Bischof WF, Frost BJ. 1998. Common reference frame for neural coding of translational and rotational optic flow. *Nature* 392:278–282.
- Wylie DRW, Winship IR, Glover RG. 1999. Projections from the medial column of the inferior olive to different classes of rotation-sensitive Purkinje cells in the flocculus of pigeons. *Neurosci Lett* 268:97–100.
- Wylie DRW, Brown MR, Barkley RR, Winship IR, Todd KG. 2003. Zonal organization of the vestibulocerebellum in pigeons (*Columba livia*): II. Projections of the rotation zones of the flocculus. *J Comp Neurol* 456: 140–153.
- Yamamoto M. 1978. Localization of rabbit's flocculus Purkinje cells projecting to the cerebellar lateral nucleus and the nucleus prepositus hypoglossi investigated by means of the horseradish peroxidase retrograde axonal transport. *Neurosci Lett* 7:197–202.
- Yamamoto M, Shimoyama I. 1977. Differential localization of rabbit's flocculus Purkinje cells projecting to the medial and superior vestibular

nuclei, investigated by means of the horseradish peroxidase retrograde axonal transport. *Neurosci Lett* 5:279–283.

Zar JH. 1999. *Biostatistical analysis*, 4th ed. Englewood Cliffs, NJ: Prentice-Hall.

APPENDIX A. Tests of Independence of Distributions of Cells between Injection Sites¹

Case	$d_{\max(k,n)}$	<i>P</i>
rVA-1	$d_{\max(10,45)} = 11$	0.088
rVA-2	$d_{\max(10,137)} = 36$	<0.001
rVA-3	$d_{\max(10,56)} = 34$	<0.001
rVA-4	$d_{\max(10,461)} = 145$	<0.001
rH45-1	$d_{\max(10,113)} = 63$	<0.001
rH45-2	$d_{\max(10,175)} = 32$	<0.001
rH45-3	$d_{\max(10,642)} = 70$	<0.001
rH45-4	$d_{\max(10,455)} = 397$	<0.001

¹Empirical Kolmogorov-Smirnov values, $d_{\max(k,n)}$, for comparisons of cell distributions across the 10 sections of the mcIO between injection zones, where there are *k* sections and *n* cells. *P* values were determined by comparing the empirical values with K-S test statistics from 1,000 randomizations of the data under the null hypothesis (which was that the two injection sites had the same distribution across the sections following the same formula as a standard test of independence).

APPENDIX B. Effect of Injection Site on Average Location of Labeled Cells¹

Case	Mean		<i>t</i>	<i>df</i>	<i>P</i>
	Zone 2 injection	Zone 0 injection			
rVA-1	3.43	2.59	2.4	35.027	0.02
rVA-2	5.36	4.15	4.02	134.619	<0.0001
rVA-3	4.36	4.98	-1.12	17.537	0.28
rVA-4	3.52	3.31	1.22	303.427	0.22
Zone 3 injection Zone 1 injection					
rH45-1	7.49	8.2	-2.27	48.894	0.03
rH45-2	5.23	7.14	-7.76	171.951	<0.0001
rH45-3	4.81	5.63	-4.41	607.036	<0.0001
rH45-4	4.52	6.07	3.89	33.132	<0.0005

¹Mean location in the series of sections between the two injection zones. Higher numbers represent more rostral locations in the mcIO. Welch's *t*-tests were used because of their greater robustness with regard to violations of assumptions than the nonparametric Mann-Whitney U tests.